Journal of Bioenergetics and Biomembranes, Vol. 35, No. 5, October 2003 (© 2003)

Mutagenesis Studies of the F_1F_0 ATP Synthase *b* Subunit Membrane Domain

Andrew W. Hardy,[1] Tammy Bohannon Grabar,[1] Deepa Bhatt,[1] and Brian D. Cain[1,2]

Received April 21, 2003; accepted May 29, 2003

A homodimer of *b* subunits constitutes the peripheral stalk linking the F_1 and F_0 sectors of the *Escherichia coli* ATP synthase. Each *b* subunit has a single-membrane domain. The constraints on the membrane domain have been studied by systematic mutagenesis. Replacement of a segment proximal to the cytoplasmic side of the membrane had minimal impact on F_1F_0 ATP synthase. However, multiple substitutions on the periplasmic side resulted in defects in assembly of the enzyme complex. These mutants had insufficient oxidative phosphorylation to support growth, and biochemical studies showed little F_1F_0 ATPase and no detectable ATP-driven proton pumping activity. Expression of the $b_{N2A,T6A,Q10A}$ subunit was also oxidative phosphorylation deficient, but the $b_{N2A,T6A,Q10A}$ protein was incorporated into an F_1F_0 complex. Single amino acid substitutions had minimal reductions in F_1F_0 ATP synthase function. The evidence suggests that the *b* subunit membrane domain has several sites of interaction contributing to assembly of F_0, and that these interactions are strongest on the periplasmic side of the bilayer.

KEY WORDS: F_1F_0 ATP synthase; *b* subunit; random mutagenesis; F_0 proton translocation.

INTRODUCTION

F_1F_0 ATP synthases are complex multimeric enzymes catalyzing the central metabolic function of ATP production in most organisms (Boyer, 1997; Capaldi and Aggeler, 2002; Senior *et al.*, 2002). In the *Escherichia coli* enzyme, the F_1 sector consists of five different subunits ($\alpha_3\beta_3\gamma\delta\varepsilon$) housing the three catalytic sites at interfaces between the α and β subunits. The F_0 sector has three intrinsic membrane subunits (ab_2c_{10}) and conducts protons across the membrane (Fillingame and Dmitriev, 2002). Electron microscopy showed that the principal mass of F_1 is connected to F_0 by two slender stalk structures (Wilkens, 2000; Wilkens *et al.*, 2000). Proton translocation through a channel in the *a* and *c* subunits drives rotation of the ring of *c* subunits and in turn the rotary stalk γ and ε subunits (Noji and Yoshida, 2001). Movement of the rotor results in sequential conformational changes in the catalytic sites of the $\alpha_3\beta_3$ hexamer accounting for the three states of the Binding Change Mechanism (Boyer, 1997; Senior *et al.*, 2002). The function of the peripheral stalk is to act as a stator holding the $\alpha_3\beta_3$ hexamer in opposition to rotation.

The primary constituents of the stator are the $b_2\delta$ subunits (McLachlin *et al.*, 1998; Rodgers and Capaldi, 1998). The δ subunit was seen perched atop F_1(Wilkens *et al.*, 2000), but recent evidence suggested that it may be involved in a specific interaction with a single α subunit (Weber *et al.*, 2003). Physical studies of the *b* subunit indicated a largely α-helical protein in an extended conformation (Cain, 2000; Dunn *et al.*, 2000; Revington *et al.*, 2002; Vogel, 2000). The b_2 homodimer stretches from the periplasmic side of the membrane to near the top of F_1 where it makes contact with the δ subunit. Additional interactions were detected between subunit *b* and at least one $\alpha\beta$ pair (McLachlin *et al.*, 2000). The combined protein–protein interactions between b_2 and the F_1 subunits provide sufficient binding energy to prevent rotation of the $\alpha_3\beta_3$ hexamer (Cherpanov *et al.*, 1999;

[1] Department of Biochemistry and Molecular Biology, University of Florida, Gainesville, Florida.

[2] To whom correspondence should be addressed; e-mail: bcain@biochem.med.ufl.edu.

0145-479X/03/1000-0389/0 © 2003 Plenum Publishing Corporation

Weber *et al.*, 2003). Dunn and coworkers have defined two distinct functional domains proximal to the carboxyl terminus necessary for formation of the b_2 dimer and interactions with F_1(Revington *et al.*, 1999). Recently, they reported the structure of the dimerization domain (Del Rizzo *et al.*, 2002). The tether region roughly corresponds to the peripheral stalk seen linking $F_1$and F_0 in electron micrographs. Relatively large insertions and deletions have been constructed in the tether region that allow retention of F_1F_0 ATP synthase activity suggesting a highly flexible structure (Sorgen *et al.*, 1998; Sorgen *et al.*, 1999), and there appear to be few inter-subunit interactions in the tether domain. However, several chemical crosslinks have been demonstrated between a cytoplasmic loop of the *a* subunit and the *b* subunit (Long *et al.*, 1998; McLachlin *et al.*, 2000). Mutations affecting *arg-36* yielded an uncoupled phenotype suggesting an altered proton channel (Caviston *et al.*, 1998).

The membrane-spanning region, residues 4-22, of the *b* subunit has not been intensively studied. Although several mutant searches and site-directed mutagenesis studies have been conducted, only a single substitution of b_{G9D} located near the periplasmic surface of the membrane yielded a strong F_1F_0 ATP synthase deficient phenotype (Porter *et al.*, 1985). Selection of second site suppressors for the b_{G9D} mutation suggested interactions between the *b* subunit and either *a* or *c* subunits that influenced the proton channel. Dmitriev *et al.* (1999) determined the structure of a polypeptide modeling the *b* subunit membrane domain in an organic solvent by nuclear magnetic resonance spectroscopy. The polypeptide formed an α-helix with a 20° bend resulting from *pro-27* and *pro-28* located near the cytoplasmic surface of the membrane. A series of cysteine substitutions within the membrane domain suggested that disulfide bridges could be most efficiently formed within the b_2 dimer at positions proximal to the periplasmic side of the membrane. This led Dmitriev *et al.* (1999) to formulate a structural model in which the extreme amino-terminal ends of the *b* subunits participated in direct interactions, but the two subunits flared apart from one another as the proteins crossed the membrane.

One of the major predictions of such a model is that amino acid substitutions in the *b* subunit proximal to the periplasmic side of the membrane might be expected to yield a more pronounced phenotype than those on the cytoplasmic side. Here we report a systematic mutational analysis of the membrane domain of the *b* subunit. The properties of the current collection of mutations support the model in which most of the important subunit interactions occur near the periplasmic side of the membrane.

EXPERIMENTAL PROCEDURES

Bacterial Strains and Growth Conditions

The *uncF (b)* gene deletion strain KM2 (Δ*b)* of *E. coli* and *b* subunit expression plasmid pKAM14 (*b*) have been described previously (McCormick *et al.*, 1993; McCormick and Cain, 1991). The media were either Minimal A supplemented with succinate (0.2% w/v) or LB supplemented with glucose (0.2% w/v) (Miller, 1992). Ampicillin (100 μg/mL) was used to maintain the plasmids, and isopropyl-1-thio-β-D-galactoside (IPTG) (40 μg/mL) was included to induce maximal expression of *b* subunit proteins. Cultures were incubated at 37°C. Bacterial culture media supplies were purchased from Difco, and supplementary chemicals and antibiotics were obtained from Sigma.

Recombinant DNA Methods

Plasmid pAWH5 (b_{6his}) was constructed from pKAM14 in several steps (Fig. 1). The amino-terminal *his*-tag was brought in from plasmid pTAM37 (Grabar and Cain, in press). Site-directed mutagenesis using the QuikChange kit (Stratgene) was employed to install additional restriction sites. The oligonucleotides were 5′ CGCAACAATCCTTGGCCAGGCAATTGCGTTTGTC CTGTTC and 5′ GAACAGGACAAACGCAATTGCC TGGCCAAGGATTGTTGCG with the underlined bases specifying the new unique *Msc*I and *Mun*I/*Mfe*I sites. These sites along with a vector *Sph*I site upstream of the *uncF(b)*-gene-coding sequence and an existing *Sna*BI site within the gene were used to generate mutations in the codons encoding the membrane spanning segment of the *b* subunit. The restriction sites used to generate mutations in plasmid pAWH5 (b_{6his}) have been summarized in Fig. 1. Mutagenic oligonucleotides were phosphorylated using T4 polynucleotide kinase and then annealed forming double-stranded synthetic DNAs. These were designed with the appropriate ends to allow direct ligation into pAWH5 (b_{6his}) digested with the restriction endonucleases. Restriction digestion, oligonucleotide phosphorylation, and ligation were performed according to the conditions specified by the suppliers (Life Technologies and New England Biolabs). Inclusion or elimination of restriction sites were used as an initial indication of successful construction of mutations, and the nucleotide sequences of all recombinant *uncF(b)* genes were directly confirmed by the Interdisciplinary Center for Biotechnology Research DNA sequencing core facility at the University of Florida.

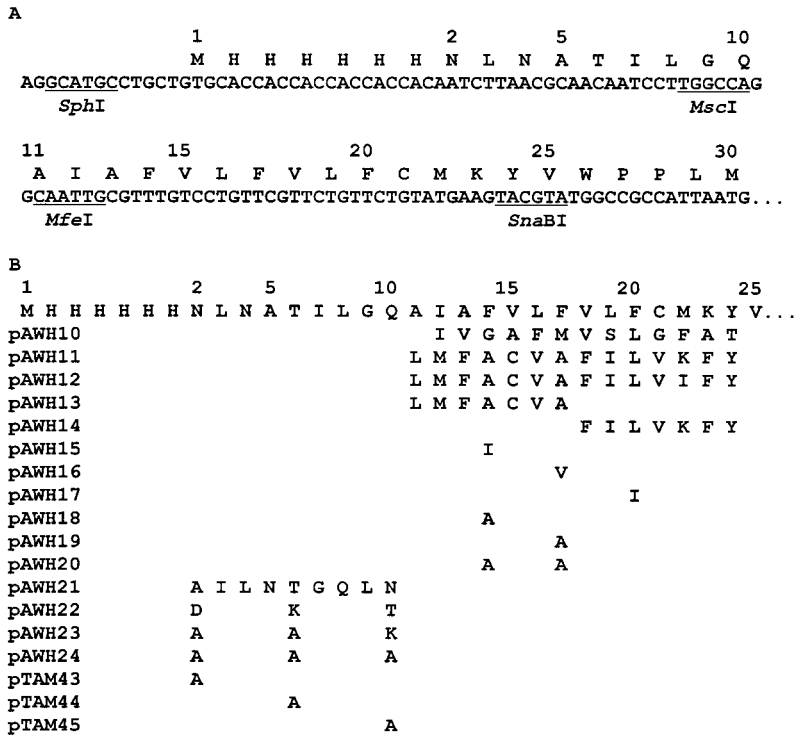

Fig. 1. Construction of *b* subunit membrane domain mutations. Amino acid substitutions were constructed by cassette site-directed mutagenesis of plasmid pAWH5 (b_{6his}). Panel A shows the coding strand nucleotide sequence, the corresponding primary protein structure and the position of restriction endonuclease recognition sequences for the membrane domain of the *b* subunit. The numbering system reflects the wild type *b* subunit primary sequence ignoring the histidine tag. Panel B plots the amino acid replacements encoded in the mutated plasmids relative to the sequence of plasmid pAWH5 (b_{6his}) (top line). For clarity only the amino acids specified by incorporation of a mutagenic oligonucleotide are shown in the figure. The mutant plasmids were identical to plasmid pAWH5 (b_{6his}).

Preparation of Membranes

Membrane vesicles were prepared essentially as described previously (Caviston *et al.*, 1998). *E. coli* strain KM2 (Δb) was transformed with pAWH5 (b_{6his}) or its derivatives. Cultures were grown to a density of approximately $OD_{600} = 1.0$. The cells were harvested by centrifugation (12,000 $\times$ *g*, 10 m) and washed in TM buffer (50 mM Tris-HCl, 10 mM $MgSO_4$, pH 7.5). The pellet was suspended in TM buffer containing DNase (10 μg/mL), and then the cells were disrupted by passage through a French Pressure Cell (SLM Instruments) at 14,000 psi. Unbroken cells and debris were removed by two successive centrifugation steps (7700 $\times$ *g*, 10 m). Membranes were collected using a Beckman Coulter LE-80K Ultracentrifuge equipped with a 70.1 Ti rotor (150,000 $\times$ *g*, 1.5 h), and then washed with TM buffer (150,000 $\times$ *g*, 1 h). The membranes vesicles were suspended using a glass homogenizer prior to use. Membrane protein was determined by the bicinchonic acid (BCA) assay (Smith *et al.*, 1985).

Activity Assays

ATP hydrolysis activity in membrane samples was determined following release of inorganic phosphate from ATP by the acid molybdate method (Sorgen *et al.*, 1999). Reactions were performed on membranes containing 60 μg of protein in 4 mL of assay buffer (50 mM Tris-HCl, 1 mM $MgCl_2$, pH 9.1) prewarmed to 37°C. The reaction was started by addition of ATP (80 μL of 150 mM ATP in 25 mM Tris-HCl, pH 7.5). ATP- and NADH-driven proton pumping assays were conducted as described previously (Sorgen *et al.*, 1998). Antibodies and immunoblot analyses were performed according to established protocols (Caviston, *et al.*, 1998).

RESULTS

Very few mutations in the membrane domain of the *b* subunit were known to significantly alter F_1F_0 ATP synthase activity. In order to define the structural requirements for the membrane spanning region, a series of plasmids expressing a set of mutations designed to systematically study the primary structural requirements of the membrane domain have been constructed. All mutant plasmids were based upon pAWH5 (b_{6his}). This plasmid was constructed with an *Sph*I site upstream of the *uncF(b)* gene, silent mutations adding *Msc*I and *Mfe*I sites within the membrane domain coding sequence, and a *Sna*BI restriction site immediately 3′ with respect to the membrane domain codons (Fig. 1(A)). Mutations were constructed by cassette-site-directed mutagenesis using double-stranded oligonucleotides. The plasmids generated for the these experiments and their amino acid replacements are shown in Fig. 1(B). The *his*-tag on the *b* subunit had no apparent affect on enzyme assembly or function (Table I).

Table I. Growth Properties and Membrane-Associated ATPase Activity of Strain KM2 Carrying *uncF(b)* Subunit Mutation Plasmids

Plasmid	Subunit	Colony size[a]	ATP hydrolysis[b]
none	Δb	−	0.11 ± 0.04
pBR322	Δb	−	0.17 ± 0.02
pKAM14	b	+ + +	1.46 ± 0.03
pAWH5	(b_{6his})	+ + +	1.48 ± 0.31
pAWH10	$b_{cox11–24}$	−	ND
pAWH11	$b_{11–24}$	−	0.44 ± 0.08
pAWH12	$b_{11–24I}$	−	0.50 ± 0.18
pAWH13	$b_{11–17}$	−	0.18 ± 0.07
pAWH14	$b_{18–24}$	+ + +	0.99 ± 0.16
pAWH15	b_{F14I}	+ + +	1.05 ± 0.33
pAWH16	b_{F17V}	+ + +	1.12 ± 0.32
pAWH17	b_{F20I}	+ + +	1.03 ± 0.12
pAWH18	b_{F14A}	+ + +	0.98 ± 0.11
pAWH19	b_{F17A}	+ + +	1.02 ± 0.00
pAWH20	$b_{F14A,F17A}$	+ + +	1.04 ± 0.06
pAWH21	$b_{2–10}$	−	0.40 ± 0.10
pAWH22	$b_{N2D,T6K,Q10T}$	−	0.56 ± 0.32
pAWH23	$b_{N2A,T6A,Q10K}$	−	0.78 ± 0.33
pAWH24	$b_{N2A,T6A,Q10A}$	−	0.83 ± 0.09
pTAM43	b_{N2A}	+ + +	1.49 ± 0.09
pTAM44	b_{T6A}	+ + +	1.13 ± 0.07
pTAM45	b_{Q10A}	+ + +	1.15 ± 0.04

[a] Colony size in excess of 1 mm on minimal A medium (+ + +), no growth (−).

[b] ATP hydrolysis expressed as μM Pi released per minute per milligram membrane protein ± standard deviation. Assays were performed in duplicate independently on at least two different membrane preparations.

Random Mutagenesis of $b_{11–24}$

The structural model developed by Dmitriev *et al.* (1999) suggested that the two *b* subunits were in close contact near their amino termini, but the transmembrane spans separated as they moved toward the cytoplasmic leaflet of the membrane bilayer. Moreover, the only single substitution known to inactivate F_1F_0 ATP synthase was b_{G9D} located near the periplasmic surface of the membrane. This suggested that there might be few structural constraints for the portion of the *b* subunit within the membrane bilayer extending from *ala-11* to *tyr-24*, aside from the necessity for maintaining an appropriate length and hydrophobic character. To test this hypothesis, plasmids expressing subunits replacing $b_{11–24}$ with heterologous sequences were studied (Fig. 1). Plasmid pAWH10 ($b_{cox11-24}$) replaced *ile-12*-to-*tyr-24* with a primary sequence modeled on a section of the membrane spanning segment of mammalian cytochrome oxidase subunit *VIc*. This particular segment was chosen because the structure of subunit *VIc* has been determined at high resolution (Tsukihara *et al.*, 1996). Subunit *VIc* has a single-membrane domain known to participate in protein–protein interactions within a multimeric-membrane complex. Plasmid pAWH11 ($b_{11–24}$) was constructed using a randomized amino acid sequence from the *b* subunit. There was concern that the lysine at position 22 of the randomized sequence might alter hydrophobicity, so an additional plasmid pAWH12 ($b_{11–24I}$) was made with isoleucine at position 22. Each of the plasmids were transformed into *uncF(b)* subunit deletion strain KM2 and F_1F_0 ATP synthase assessed. None of these large multiple residue replacements in the interior membrane domain of the *b* subunit resulted in a functional F_1F_0 ATP synthase. The transformants failed to grow on succinate medium showing defects in oxidative phosphorylation (Table I). Studies of membrane-associated F_1F_0 ATPase-mediated ATP-driven proton pumping in isolated membrane vesicles revealed little or no coupled enzyme function (Fig. 2). In each case, NADH driven fluorescence quenching was followed to demonstrate intact membrane vesicles (data not shown). The ATP hydrolysis assays were performed under conditions that release F_1-ATPase from the influence of mutations in F_0, so the low level of F_1F_0 ATPase activity suggested a defect in assembly and stability of the enzyme complex (Table I).

The random sequences were then divided in half during construction of pAWH13 ($b_{11–17}$) and pAWH14 ($b_{18–24}$). Plasmid pAWH13 ($b_{11–17}$) KM2 transformants were again fully defective (Fig. 2, Table I). In contrast, KM2/pAWH14 ($b_{18–24}$) grew well on succinate

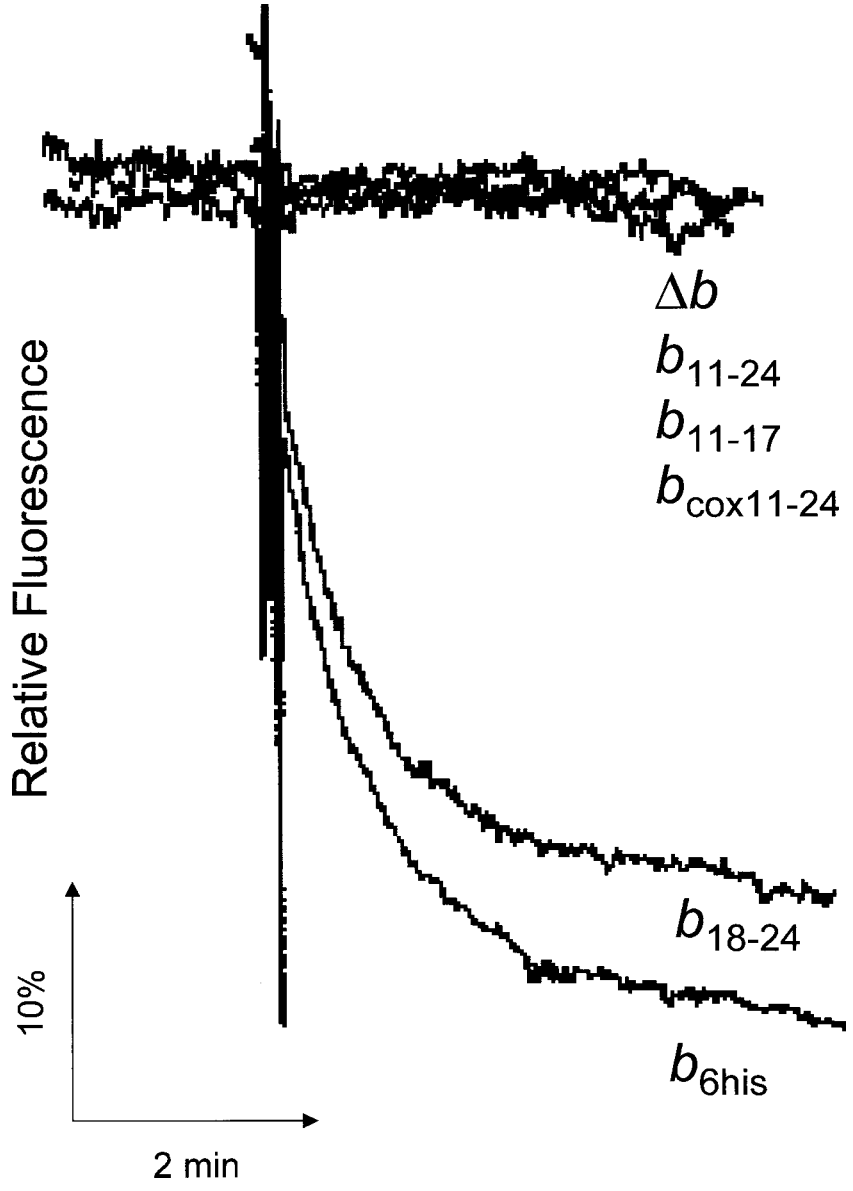

Fig. 2. ATP-driven energization of membrane vesicles prepared from *b* subunit membrane domain mutants. Membrane vesicles (250-μg protein) were suspended in 3 mL assay buffer (50 mM 4-morpholinepropanesulfonic acid (MOPS), 10 mM $MgCl_2$, pH 7.3) and the reaction started by addition of ATP (0.4 mM). The fluorescence of 9-amino-6-chloro-2-methoxyacridine was recorded with excitation at 410 nm and emission at 490 nm. Traces: Δb, membranes from strain KM2 (Δb); $b_{11–24}$, KM2/pAWH11; $b_{11–17}$, KM2/pAWH13;$b_{cox11–24}$, KM2/pAWH10; KM2/pAWH12 $b_{18–24}$, KM2/pAWH14; b_{6his}, KM2/pAWH5.

medium, and membranes prepared from these cells had considerable amounts of intact and active F_1F_0 ATP synthase. The levels of ATP-driven proton pumping activity in isolated membranes approached the activity seen in the positive control KM2/pAWH5 (b_{6his}) membranes (Fig. 2). These results suggested that a series of hydrophobic amino acids was indeed sufficient for the segment of the transmembrane domain from positions 18 to 24.

One of the features of the membrane spanning segment of the *b* subunit were a series of three phenylalanines spaced such that they would stack along one face of an α-helix. Two, *phe-14* and *phe-17*, were among the amino

acids replaced in randomized $b_{11–17}$ sequence, and *phe-14* was highly conserved in bacterial *b* subunit membrane segments. Therefore, the membrane segment phenylalanines were targeted for mutagenesis to detect functional constraints associated with the aromatic amino acids. Plasmids were constructed to substitute *phe-14*, *phe-17*, and *phe-20* alone or in combination with alanine and larger hydrophobic amino acids. All plasmids including the double mutant plasmid pAWH20 ($b_{F14A, F17A}$) complemented KM2 for growth on succinate medium (Table I). Membranes prepared from all cells expressing the various phenylalanine replacements displayed abundant coupled F_1F_0 ATPase activity (Table 1).

Mutagenesis of $b_{2–10}$

Crosslinking studies had suggested close association between the amino terminal regions of the two *b* subunits at the periplasmic surface of the membrane (Dmitriev *et al.*, 1999). This suggested that substitutions in area of the *b* subunit proximal to the periplasmic side of the membrane might result in defective F_1F_0 ATP synthases. The initial experiment designed to address the extreme amino terminal segment of the *b* subunit was to randomize the primary sequence from *asn-2* through *asn-10.* As expected, the *b* subunit with a randomized sequence expressed in KM2/pAWH21 ($b_{2–10}$) resulted in loss of enzyme function (Table I).

Two plasmids were constructed to focus on the three amino acids that had shown the strongest crosslinking activity suggesting close interaction between the two *b* subunits. Plasmid pAWH22 ($b_{N2D,T6K,Q10T}$) replaced the polar amino acids at positions 2, 6, 10, with other polar amino acids. Plasmid pAWH24 ($b_{N2A,T6A,Q10A}$) was an alanine scan of the same three positions. Both plasmids failed to complement deletion strain KM2 (Table I). Surprisingly, the defects appeared to occur through different mechanisms. Neither set of membrane preparations had coupled ATP-driven proton translocation (Fig. 3). However, the substitution of polar amino acids resulted in a sharp reduction in membrane associated ATP hydrolysis activity, while replacements with alanine yielded relatively high level of activity. The latter result suggested assembly of an intact but nonfunctional F_1F_0 complex in strain KM2/pAWH24 ($b_{N2A,T6A,Q10A}$). Since *b* subunit that has not been incorporated into an F_1F_0 complex is labile in vivo, the amount of *b* subunit in the membrane was employed as a second indicator of assembled F_1F_0. Immunoblot analysis revealed very low levels of either $b_{2–10}$ or $b_{N2D,T6K,Q10T}$ proteins in membranes from *E. coli* (Fig. 4). A much higher amount of $b_{N2A,T6A,Q10A}$ subunit was found. The level rivaled that detected in membranes from KM2/pAWH14 ($b_{18–24}$) which has sufficient F_1F_0 ATP synthase for essentially wild-type growth properties. Apparently, the $b_{N2A,T6A,Q10A}$ subunit was efficiently assembled into a F_1F_0 complex, but was incapable of assuming a conformation suitable for coupled proton translocation.

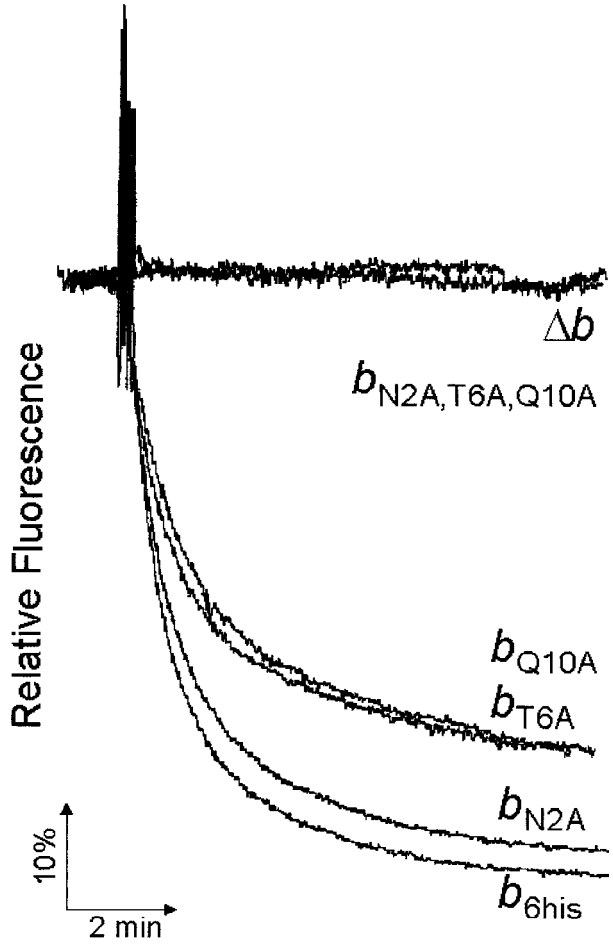

Fig. 3. ATP-driven energization of membrane vesicles prepared from *b* subunit membrane domain mutants. ATP-driven proton pumping activity was determined as described in Fig. 2. Traces: Δ*b*, membranes from strain KM2/pBR322 (Δ*b*); $b_{N2A,T6A,Q10A}$, KM2/pAWH24; b_{N2A}, KM2/pTAM43; b_{T6A}, KM2/pTAM44; b_{Q10A}, KM2/pTAM45; b_{6his}, KM2/pAWH5.

In view of this observation, we considered whether any of the individual alanine replacements was sufficient to generate a discernable phenotype. Mutations specifying the b_{N2A}, b_{T6A}, and b_{Q10A} substitutions were constructed in plasmids pTAM43, pTAM44, and pTAM45, respectively. All three complemented strain KM2, and the membranes displayed high levels of enzyme function in biochemical assays (Table I, Fig. 4).

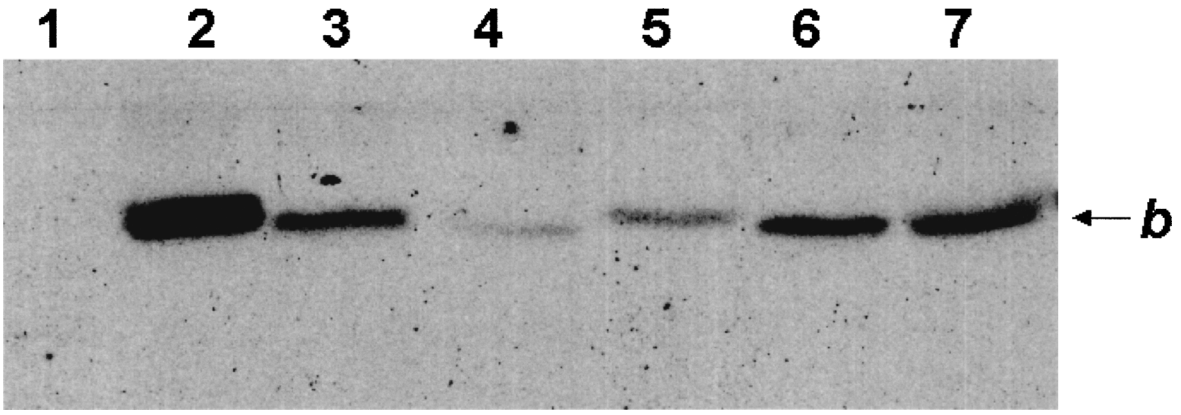

Fig. 4. Immunoblot analysis of membranes prepared *b* subunit membrane domain mutants. Membrane proteins (20 μg) were separated using a 15% *bis*-acrylamide gel, and then transferred to nitrocellulose. Immunodetection using an anti-*b* subunit polyclonal antibody was achieved as described by Caviston *et al.* (1998). Lanes: lane1, strain KM2 (Δb); lane 2, KM2/pAWH5 (b_{6his}); lane 3, KM2/pAWH23 ($b_{N2A,T6A,Q10k}$); lane 4, KM2/pAWH22 ($b_{N2D,T6K,Q10T}$); lane 5, KM2/pAWH21 ($b_{2–10}$); lane 6, KM2/pAWH24 ($b_{N2A,T6A,Q10A}$); lane 7, KM2/pAWH14 ($b_{18–24}$).

DISCUSSION

In this paper we report the first systematic mutational survey of the membrane domain of the *b* subunit of the *E. coli* F_1F_0 ATP synthase. Replacement of the entire membrane domain with either the structurally defined membrane domain of cytochrome oxidase subunit VIc or a sequence containing the randomized amino acids from the *b* subunit membrane domain resulted in loss of F_1F_0 ATP synthase activity. This established that there were specific sequence requirements for the *b* subunit membrane domain. This simple statement was important because several mutant searches and site-directed mutagenesis studies yielded only a single substitution, b_{G9D}, with a marked F_1F_0 ATP synthase deficient phenotype (Porter *et al.*, 1985). However, sequence specificity apparently does not extend to the segment of *val 18–tyr 24* because limiting the amino acid substitutions to this segment yielded a *b* subunit that was both efficiently assembled into the enzyme complex and functional. Multiple amino acid substitution mutations targeted to positions more proximal with respect to the amino terminus, *asn-2–ala-17*, of the subunit resulted in enzyme failure. The defects resulting from substitutions were generally associated with a failure to assemble the F_1F_0 enzyme complex. In contrast, the $b_{N2A,\ T6A,\ Q10A}$ subunit appeared to be incorporated into an intact, nonfunctional F_1F_0 complex. The evidence suggests that the amino-terminal section of the membrane domain was far more sensitive to manipulation than the area on the cytoplasmic side of the membrane.

The collection of mutations can be interpreted as support for the structural model in which the amino termini of the two *b* subunits are in contact, and then the two separate spatially as the membrane is crossed. Although the dimerization domain provides much of the binding energy for formation of the b_2 homodimer (Dunn *et al.*, 2000), studies indicated that protein–protein interactions within the *b* subunit membranes domain also contributed to F_1F_0 ATP synthase assembly. Our research suggests that these additional interactions occur in the area of the segment of the *b* subunit spanning the periplasmic leaflet of the cytoplasmic membrane. The strongest of these interactions may occur close to the surface of the membrane rather than deep within the membrane. The properties of the $b_{N2A,\ T6A,\ Q10A}$ subunit were most interesting in this respect. Apparently, there were sufficient inter-subunit contacts to support assembly, but the F_0 proton channel was not functional. This observation has important implications with respect to proton channel. The result supports the idea that the *b* subunit membrane domain plays a necessary structural role in aligning the channel-forming-membrane domains of the *a* and *c* subunits. This is probably the basis for the requirement for a *b* subunit membrane domain in reconstitution of the F_0 proton channel (Greie *et al.*, 2000). It is notable that *a* and *c* subunit second site suppressor mutations for b_{G9D} partially restored proton translocation without improving F_0 assembly (Kumamoto *et al.*, 1987). Mutations affecting the immediate amino-terminal segment of the *b* subunit apparently result in a structural defect propagated into the interface between the stator and rotor within F_0. A defect of this nature might be expected to either restrict the entry to the H^+ channel or prevent free rotation of the ring of *c* subunits.

The normal growth phenotypes of cells expressing the single mutation b_{N2A}, b_{T6A}, and b_{Q10A} subunits on F_1F_0 ATP synthase mirrored cysteine replacement mutations at

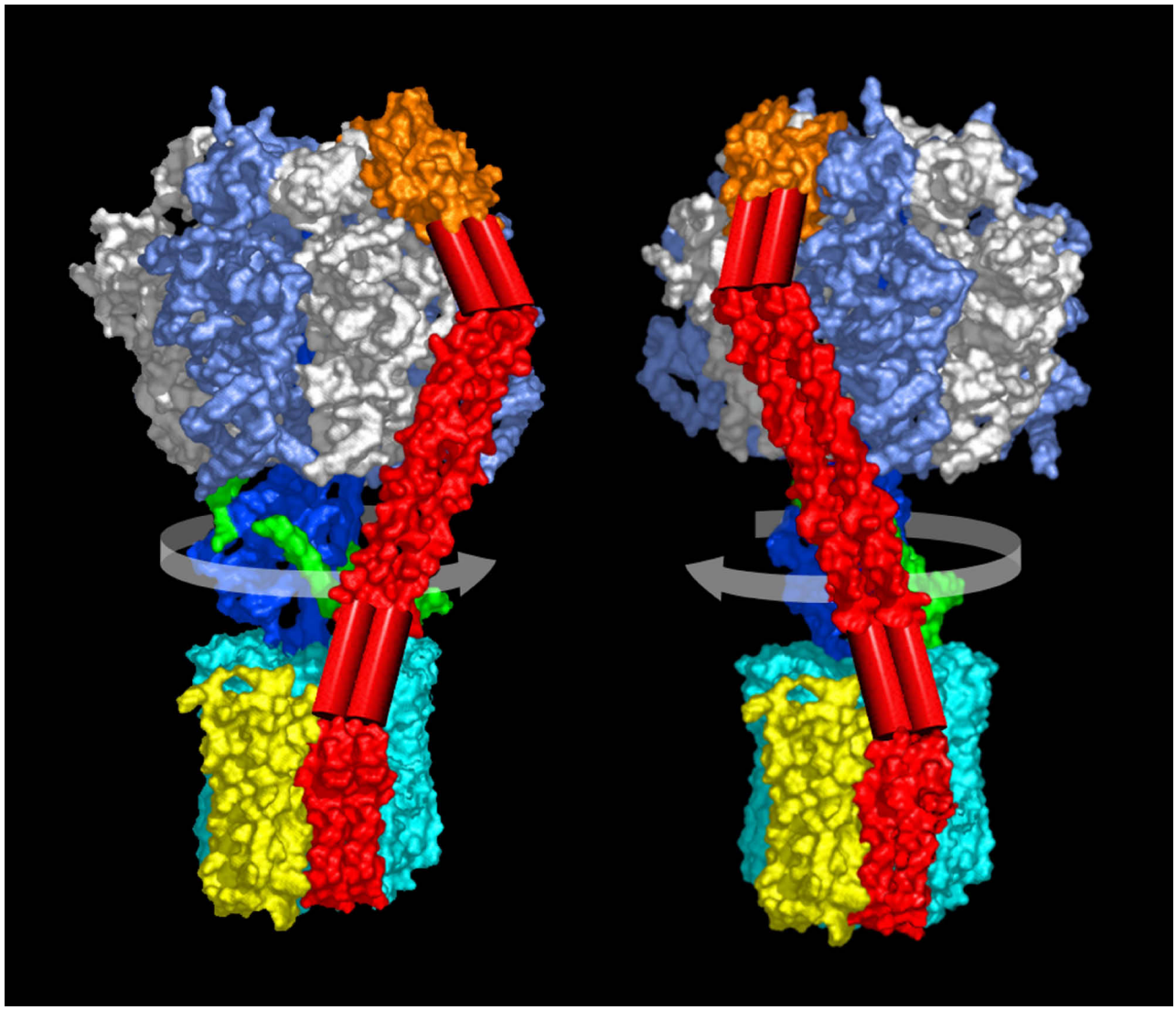

Fig. 5. Model for stator reorientation depending upon the direction of rotation. The panel on the left represents the position of the b_2 dimer during ATP synthesis, and the panel on the right shows the enzyme during ATP hydrolysis. The arrows indicate the direction of rotation of the rotary stalk subunits ($\gamma\varepsilon c_{10}$). The cylinders indicate areas of the *b* subunits for which no high resolution structure has been determined. The subunits are colored as follows: *a*, yellow; *b*, red; *c*, cyan; α, light blue; β gray; γ, blue; δ, orange; ε, green.

the same positions (Dmitriev *et al.*, 1999). The latter collection also displayed no growth phenotypes using succinate as a carbon source. Similarly, replacement of the conserved phenylalanines had little impact on function. Certainly the minimal loss of enzyme function associated with any of the individual mutations did not appear to add up to the failure associated with the combined $b_{N2A,T6A,Q10A}$ subunit. This would seem to argue that while no single position is essential to the interactions needed to assemble a functional F_0, several sites of interaction from the amino terminus through to *phe-17* contribute to establishing the appropriate subunit contacts within F_0.

The research presented here suggests little interaction between the two *b* subunits as the protein exits the bilayer on the cytoplasmic side of the membrane. This segment of the b_2 dimer might be expected to be highly flexible unlike areas of close interaction, such as the dimerization domain. Moreover, F_1F_0 ATP synthase function has been demonstrated for enzymes with altered lengths of the tether domains above the membrane surface (Sorgen *et al.*, 1998, 1999), and this is again consistent with a highly flexible section of the b_2 dimer. Indeed the tether domains of two *b* subunits need not be the same length for formation of an F_1F_0 complex (Grabar and Cain, 2003).

The question arises as to why should there be so much flexibility in the element of the enzyme designed to function as the principal constituent of the stator? Perhaps this highly flexible segment of the b_2 dimer serves as a hinge allowing reorientation of the stator depending on the direction of rotation as the enzyme carries out ATP synthesis or hydrolysis (Fig. 5).

ACKNOWLEDGMENTS

Research reported in this paper was included in a thesis by AWH in partial fulfillment of the requirements for the Master of Science degree. The authors thank Mr Nathan Bryant for his invaluable assistance in the preparation of Fig. 5. The work was supported by Public Health service Grant No. RO1 GM43495 (BDC).

REFERENCES

Boyer, P. D. (1997). *Annu. Rev. Biochem.* **66**, 717–749.
Cain, B. D. (2000). *J. Bioenerg. Biomembr.* **32**, 365–371.
Capaldi, R. A., and Aggeler, R. (2002). *Trends Biochem. Sci.* **27**, 154–160.
Caviston, T. L., Ketchum, C. J., Sorgen, P. L., Nakamoto, R. A., and Cain, B. D. (1998). *FEBS Lett.* **429**, 201–206.
Cherpanov, D. A., Mulkidjanian, A. Y., and Junge, W. (1999). *FEBS Lett.* **449**, 1–6.
Del Rizzo, P. A., Bi, Y., Dunn, S. D., and Shilton, B. H. (2002). *Biochemistry* **37**, 347–355.
Dmitriev, O., Jones, P. C., Jiang, W., and Fillingame, R. H. (1999). *J. Biol. Chem.* **274**, 15598–15604.
Dunn, S. D., Revington, M., Cipriano, D. J., and Shilton, B. H. (2000). *J. Bioenerg. Biomembr.* **32**, 347–355.
Fillingame, R. H., and Dmitriev, O. (2002). *Biochim. Biophys. Acta* **1565**, 232–245.
Grabar, T. B., and Cain, B. D. (2003). *J. Biol. Chem.* **278**, 34751–34756.
Greie, J., Deckers-Hebestreit, G., and Altendorf, K. (2000). *J. Bioenerg. Biomembr.* **32**, 357–364.
Kumamoto, C. A., and Simoni, R. D. (1987). *J. Biol. Chem.* **262**, 3060–3064.
Long, J. C., Wang, S., and Vik, S. (1998). *J. Biol. Chem.* **273**, 16235–16240.
McCormick, K. A., and Cain, B. D. (1991). *J. Bacteriol.* **173**, 7240–7248
McCormick, K. A., Deckers-Hebestreit, G., Altendorf, K., and Cain. B. D. (1993). *J. Biol. Chem.* **268**, 24683–24691.
McLachlin, D. T., Bestard, J. A., and Dunn, S. D. (1998). *J. Biol. Chem.* **273**, 15162–15168.
McLachlin, D. T., Coveny, A. M., Clark, S. M., and Dunn, S. D. (2000). *J. Biol. Chem.* **275**, 17571–17577.
Miller, J. H. (1992). In *A Short Course in Bacterial Genetics*, Cold Spring Harbor Laboratory Press, Cold Spring Harbor, New York, pp. 25.3–25.5.
Noji, H., and Yoshida, M. (2001). *J. Biol. Chem.* **276**, 1665–1668.
Porter, A. C. G., Kumamoto, C., Aldape, K., and Simoni, R. D. (1985). *J. Biol. Chem.* **260**, 8182–8187.
Revington, M., Dunn, S. D., Shaw, G. S. (2002). *Protein Sci.* **11**, 1227–1238.
Revington, M., McLachlin, D. T., Shaw, G. S., and Dunn, S. D. (1999). *J. Biol. Chem.* **274**, 31094–31101.
Rodgers, A. J. W., and Capaldi, R. A. (1998). *J. Biol. Chem.* **273**, 29406–29410.
Senior, A. E., Nadanaciva, S., and Weber, J. (2002). *Biochim. Biophys. Acta* **1553**, 188–211.
Smith, P. K., Krohn, R. I., Hermanson, G. T., Mallia, A. K., Gartner, F. H., Provenzano, M. D., Fujimoto, E. K., Goeke, N. M., Olson, B. J., and Klenk, D. C. (1985). *Anal. Biochem.* **150**, 76–85; Erratum (1987). *Anal. Biochem.* **163**, 279.
Sorgen, P. L., Bubb, M. R., and Cain, B. D. (1999). *J. Biol. Chem.* **274**, 36261–36266.
Sorgen, P. L., Caviston, T. L., Perry, R. C., Bubb, M. R., and Cain, B. D. (1998). *J. Biol. Chem.* **273**, 27873–27878.
Tsukihara, T., Aoyama, H., Yamashita, E., Tomizaki, T., Yamaguchi, H., Shinzawa-Itoh, K., Nakashima, R., Taono, R., and Yoshikawa, S. (1996). *Science* **272**, 1136–1144.
Vogel, P. D. (2000). *J. Bioenerg. Biomembr.* **32**, 413–421.
Weber, J., Muharemagic, A., Wilke-Mounts, S., and Senior, A. E. (2003). *J. Biol. Chem.* **278**, 13623–13626.
Wilkens, S. (2000). *J. Bioenerg. Biomembr.* **32**, 333–339.
Wilkens, S., Zhou, J., Nakayama, R., Dunn, S. D., and Capaldi, R. A. (2000). *J. Mol. Biol.* **295**, 387–391.